

Holographic Optics for Beamsplitting and Image Multiplication

A. L. Mikaelian, A. N. Palagushkin, and S. A. Prokopenko

Institute of Optical Neural Technologies, Russian Academy of Sciences,
No 44/2 Vavilov Str., 117333 Moscow, Russia, Phone: +7-(095)-135-5551,
Fax: +7-(095)-135-7802, E-mail: iont@glas.apc.org

Summary. This paper describes how we see the prospects for just a small part of holographic optics. In our opinion, CGHs have the best practical potential for the near future. For this reason, we concentrate on the methods in the design and manufacture of CGHs. In designing and making phase CGHs, we show that the best realization of their capabilities requires a fresh approach to such important problems as the correct choice of the number of phase relief gradations, accuracy evaluations and monitoring of the fabrication process. The results of our research are given.

1 Introduction

Today, the fast progress of holographic optics design methodology and manufacturing techniques is evident. Diffractive optical elements (DOEs) and computer-generated holograms (CGHs) have become an integral part of many advanced optical systems. Holographic optical elements (HOEs) are finding ever-widening application in such fields as pattern recognition, optical processing, communications, medicine, data storage, laser treatment of materials, optical switching and neural networks. Holographic methods are effectively used for making spectroscopic prisms, Fresnel lenses, laser resonators and microinterferometers and for correcting aberrations.

The demand for larger arrays of light sources can be met with the help of holographic laser beamsplitters and monolithic arrays of diffraction gratings and flat lenses. The advantage of flat diffraction elements with a surface phase relief is the possibility of combining a number of functions in a single element (e.g. beamsplitter, lenslet, diffraction grating and aberration corrector) and simple methods of copying (e.g. using polymer materials).

HOEs can be used not only with coherent and partially coherent (e.g. multimode laser radiation) but also with incoherent light. The latter case involves greater dispersion effects and lower coherent noise (speckle patterns). The present state of the art of HOE development is reported in general surveys [1–3, 5] and in the proceedings of the symposium OIST'97 [4] held in Moscow in 1997 (conference on computer and holographic optics).

2 Review of the Literature

The availability of powerful computers makes it possible to use extensive computational algorithms for designing and optimizing CGHs. A lot of research teams worldwide work in this field. The methods of CGH computations are considered in [5–8]. Software for the iterative calculations and analysis of CGHs is described in [8–10]. The usual result of the computations is a particular phase distribution in the CGH plane which is realized as an appropriate surface microrelief using photo- or electron lithography and ion or plasmachemical etching methods [11].

The application of optical lithography for making multilevel visible-range phase elements does not give the necessary accuracy [12,13]. Though very precise, masks written by an electron beam cannot solve the problem because of insufficiently exact alignment. The repeated use of e-beam lithography for forming each phase level gives the necessary accuracy; however, this way is rather expensive and time consuming [11,14]. Currently, the methods of direct-write e-beam [15] and laser [16–18] lithography are employed for recording halftone phase reliefs in resist (light or electron sensitive materials). The development of the latent relief takes only one exposition cycle. The most promising modern method of making multilevel phase elements seems to be the direct electron-beam writing of the multilevel relief in electron-sensitive resist [19]. The method is relatively expensive; however, once made, the element can simply be copied using polymer materials.

In addition to conventional CGHs with feature dimensions $d \gg \lambda$ elements with $d < \lambda$ (which are not diffractive elements in terms of classical optics) are also developed. Examples of such subwavelength elements are reflection and antireflection coatings and elements that can change the state of polarization. There is promising research into polarization-sensitive birefringent CGHs (BCGHs) (where phase reliefs are formed on the surface of a birefringent material) [20,21] and optoelectronic devices (VLSI) for high-speed communication systems. Optical volume hologram-based elements that are sensitive to light polarization and wavelength are used in optical communication lines as switches (free-space optical multistage interconnection network) [21–28]. A set of CGH gratings are used for exciting the zero-order mode in a planar optical waveguide [29,30].

Various combinations of CGHs with other optical elements are also a subject of today's investigations. For example, [31] describes the combination of high-efficiency radiation-resistant polarization diffraction gratings with multilayer dielectric mirrors used for wavefront correction of pulsed high-power solid-state lasers. Reference [32] offers to weakly couple a thin-film planar optical waveguide to a CGH. The resonance effects that result in that system allow the control of transmittance by slightly changing the angle of coupling.

A new line of investigation connected with the development of dynamic CGHs has recently emerged. A novel optical device – MACH (multiple active computer-generated hologram) – is proposed in [33]. The device combines

a phase CGH that can produce several output diffraction patterns with a liquid-crystal phase-shifting medium that enables the selection of a specific pattern and can be used for spatial filtering, 3-D image formation, and interconnection. However, the design has a disadvantage typical of all LC devices – slow response ($\sim 1.5 \mu\text{s}$). Acousto-optical light deflectors (AOD) [34] and programmable electrooptical phase diffraction modulators [35,36] are used in developing fast devices with switching speeds of $\sim 0.1\text{--}1 \mu\text{s}$.

As an alternative, we proposed a 2-D acousto-optical modulator that uses two perpendicular acoustic waves generated in a transparent medium and a variant design combining the deflector with a CGH (see below).

We note that research in the field of synthesized holographic optics has become more active over the past few years. The CGH capabilities and areas of application have expanded significantly. The integration of CGHs with other optical elements allowed absolutely new characteristics to be developed. The manufacturing of CGHs is beginning to depart from the conventional methods of microelectronics, concentrating on direct-write techniques and polymer copying of phase reliefs.

At present, efforts are being made to develop methods to control diffraction patterns in real time. Of these methods, dynamic electro- and acousto-optical CGHs look to be the most promising.

3 Methods of Phase Hologram Synthesis

While the methods of hologram synthesis are constantly growing in number, the ever-growing power of modern computers allows the computation and analysis of more and more complex diffractive elements.

Depending on the relation between the CGH feature, d , and the wavelength, λ , various methods of CGH synthesis and analysis are used:

- $d \gg \lambda$. The realm of paraxial Fourier optics. The scalar approximation of the diffraction theory is used. The output field is proportional to the complex transmittance function of HOEs. The transfer function is described by Fresnel and Fraunhofer integrals.
- $d \leq 10\lambda$. Methods of geometric optics are used together with Fresnel coefficients.
- $d \approx \lambda$. It is necessary to employ strict electromagnetic theory and find solutions to Maxwell's vector equations. Just a few problems have exact solutions. The number of computations is very large.
- $d \ll \lambda$. It is also necessary to use strict electromagnetic theory; however, there are approximation methods.

In most cases, the hologram synthesis can be performed with the paraxial approximation of Fourier optics ($d \gg \lambda$) and it requires consideration of such parameters as (1) the phase of working orders; (2) the efficiency (which is

to be as high as possible); and (3) the amplitude and phase of noise (higher diffraction orders, the field beyond the area of useful signal).

Any complex transmittance function can be used at the beginning of computations which are then to be optimized using a suitable technique (e.g. the gradient algorithm, annealing simulation). The inverse method is more efficient: the input field (and the corresponding transfer function $t(x, y)$) is computed using a predefined output pattern and then optimized. The iterative inverse method is used most often. The input field (and the transfer function $t(x, y)$) is computed using a predefined output pattern. The limitations that are largely defined by the material and the manufacturing method used (e.g. the uniform transmittance of the element, graded phase lag) are posed on the transfer function. The modified transfer function is then taken to find the output diffraction pattern. If the result is not satisfactory (e.g. low efficiency, great intensity variations), the required output amplitude distribution is taken to recompute the input field; during this process, the variable parameters (e.g. phase distribution) are kept fixed. The computation cycles are repeated until the result is good or the process stops. The limitations on the transfer function, $t(x, y)$, can be introduced gradually in the course of the iteration process. The fast Fourier transform algorithm is used to speed up the computations of Fresnel and Fraunhofer integrals. If necessary, the domain of signal legitimacy can be expanded to suppress noise (unintended diffraction orders) around the working diffraction orders.

Iterative methods using the phase retrieval algorithm [37] are now most effective. The limitation of the method – the discrete structure representation – approximately matches the ability of the current methods of CGH fabrication, lithography and direct electron-beam writing. The error diffusion algorithm allows lower corruption of the output distribution by modifying the transfer function. Annealing simulation, a method of nonlinear parametric optimization, is also widely used.

Direct computation of the binary structure is rather slow because each single period of practically any CGH (except for those that give the simplest output patterns) contains too many pixels. The phase encoding method is sometimes used in CGH computations.

The combined method [38] looks most promising. It includes:

- Conventional iterative algorithm (including gradual modification of the CGH transfer function). A pseudorandom noise signal whose amplitude gradually falls with iterations, can be introduced to attain the deepest minimum of the desired phase function.
- Gradient optimization of the output phase function followed by recomputation of the input field and modification of the transfer function.
- Binary search for the greatest sensitivity of the transmittance function to phase changes (e.g. at the boundaries of equiphase areas) by varying the phase of two or three pixels in a particular small area.

- Optimization of the CGH phase relief topology (smoothing the boundaries between equiphase areas) in order to increase the efficiency.
- Gradation of the continuous phase function can be accompanied by gradient optimization of the quantization threshold levels.

This method and the direct-write technique make it possible to manufacture two- to four-level CGHs with an efficiency of over 70% and beam intensity variations of less than 3%. The quantization of the phase function into more levels (over 8) is not reasonable because it makes the design and manufacturing more complicated with only minor improvements in the performance parameters.

4 CGH Design and Manufacture

The methods used in the computation and manufacture of holographic elements are closely related because many manufacturing errors can be predicted and corrected at the design stage. The result of computations is usually a large body of topological data needed for manufacturing a specific element and allowing for particular technological equipment.

4.1 Phase Function Gradation and Efficiency Evaluation

The computer synthesis methods give the continuous or gradated phase functions of a CGH. The continuous function allows better performance of the element but is rather hard to implement. Most manufacturing technologies require the gradated phase profile (of two to eight phase levels). Naturally, the gradation deteriorates the output diffraction pattern, increases the beam intensity variations and decreases efficiency. Efficiency is considered to mean the ratio of the total intensity of working-order beams to the intensity of the light incident on the CGH. We have worked out a simple method of evaluating the efficiency of gradated-phase elements.

The method is based on the representation of the stepped phase function as a superposition of the original continuous function P and phase correction function ΔP . The latter varies from $-Q/2$ to $+Q/2$ (where $Q = 2\pi/n$ is the phase difference between quantization levels, n is the number of levels). On this assumption, the effect of phase quantization on the CGH efficiency is similar to the introduction of a certain phase diffuser. It is important to note that the effect of the diffuser is dependent on the number of quantization levels rather than the phase function, no matter how complicated it may be. Pseudorandom phases of the diffuser range from $-Q/2 + C$ to $+Q/2 + C$ (where C is a constant). The scattering of light on the diffuser decreases the intensity of the zero-order beam and can be computed for each particular number of phase levels. The efficiency of a CGH with a stepped phase function, E_q , may be written as

$$E_q(n) = \eta(n) * E_c,$$

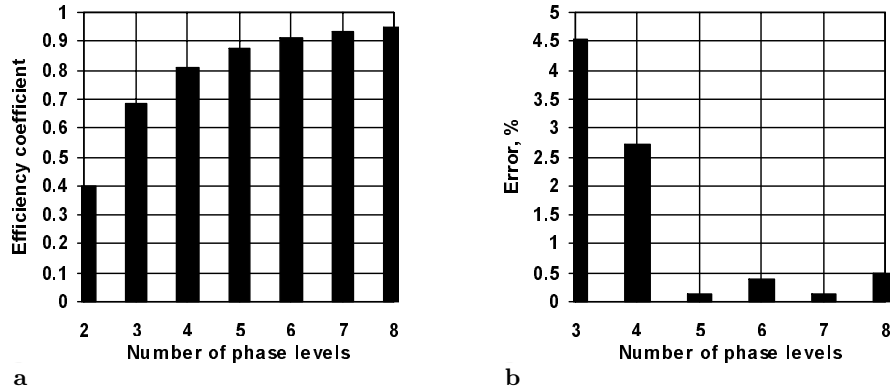


Fig. 1. (a) The relation between $\eta(n)$ and the number of phase levels for a CGH with 64×64 pixels in the period. (b) The relative error of evaluation

where E_c is the efficiency of the HOE with continuous phase function, $\eta(n)$ is the portion of the diffuser's energy in the zero-order beam.

The coefficient $\eta(n)$ is dependent on the number of phase levels and independent of the phase function itself. Figure 1a shows how $\eta(n)$ depends on the number of phase levels, n , and Fig. 1b the relative error of evaluation.

It should be noted that the method is only applicable to CGHs with originally continuous phase functions; that is, it evaluates how gradation affects the efficiency of the continuous-relief element. The result of many computation methods is a gradated phase function (see Sect. 3 and [38]). These methods make it possible to avoid the negative effects of phase gradation and manufacture even binary phase elements with an efficiency of as high as 79% (see Table 1 below).

4.2 CGH Manufacture. Specificity and Accuracy

The manufacture of phase reliefs of holographic elements must be very precise. The ion and plasmachemical etching techniques and methods of control that are used in microelectronics usually need significant improvement to provide such a high degree of accuracy.

Reference [39] gives the estimates of necessary accuracy by modeling the work of a beamsplitter with equal-intensity output beams. The criterion of the estimates was the output beam intensity variations, which should not be greater than 5%. The maximal admissible variations of equiphase pixel group boundaries and relief depth were found for different numbers of phase gradation levels. The requirements for manufacturing accuracy were shown to grow with the number of phase levels. For example, if a CGH has the index of refraction $n = 1.5$ and operates at $0.63 \mu\text{m}$, the displacements of the phase areas should not exceed 0.1% of the phase function period. For a $200\text{-}\mu\text{m}$ period, this corresponds to a $0.1\text{-}\mu\text{m}$ accuracy.

The requirements for the phase relief depth are more rigid: the variations here must not exceed 1%. For a typical value of $\sim 0.63\ \mu\text{m}$, the relief depth should be made to $\pm 0.006\ \mu\text{m}$. In practice, certain smoothing of the relief takes place in manufacturing, which results in slight defocusing and scattering of laser light. Our estimation says that if the mean variations of the relief depth do not exceed $\pm 0.01\ \mu\text{m}$, the output beam intensity variations keep within the 5% limit.

4.3 Optical Methods of Fabrication

The use of conventional optical lithography can provide, at most, 1- μm line-width resolution and 0.2- μm positioning accuracy, which is suitable only for manufacturing infrared phase elements or elements with very small angles of diffraction ($< 0.1^\circ$).

The direct laser writing of a phase relief on resist or the making of halftone masks [16–18] gives somewhat better results. The use of halftone masks solves the problem of automatic alignment of phase level boundaries because the recording and exposition require one cycle each.

4.4 Use of E-beam and Direct-write Lithography

E-beam lithography allows the drawing of masks with 0.1- μm resolution and 0.01- μm line-position accuracy. The use of such masks provides the accuracy necessary for CGH manufacturing; yet, the problems of fine alignment and low-resolution optical lithography remain. They can be solved by using halftone e-beam generated masks and deep UV for exposition.

Successive cycles of e-beam lithography and etching is another method of making phase reliefs which meet the accuracy requirements. However, this expensive method is too slow and can only be justifiably used for manufacturing highly accurate samples and production masters.

We use the technique of direct e-beam writing in which a computer synthesised phase structure is recorded into the resist layer deposited on a glass substrate [19].

The maximal depth of the phase relief here is determined by the resist layer thickness. To suppress the reflection of light at the resist–glass interface, the index of refraction of the substrate is chosen to be close to that of resist. The etching treatment with specially adjusted exposure doses and etching modes is used to obtain the desired depth of phase levels. The departure of working-order beam intensities from design values serves as an accuracy criterion. The method makes use of all of the advantages of e-beam lithography – high resolution and precise positioning. Multiple-level phase reliefs are produced in a single exposition cycle, which eliminates the mask-alignment problem. The whole process is not so time-consuming because it needs fewer manufacturing steps.

4.5 Plasmachemical Etching of Reliefs in Glass. Methods of Copying Phase Reliefs

CGHs have diverse applications, so the choice of elements depends on the specific operation conditions. CGHs that are made in electron or optical resist layers deposited on glass substrates can be used mostly in airtight optical devices because of their susceptibility to moisture. Rugged operation conditions require CGHs to be made of pure glass, quartz or transparent optical crystals without using other susceptible materials. The use of birefringent crystals is also welcome in manufacturing polarization-sensitive elements (BCGHs).

The use of wet chemical etching is impossible because of low resolution, insufficient boundary sharpness, and poor reproducibility. Only plasma etching is applicable in CGH manufacturing. In microelectronics, plasma etching is used for treating thin films of various materials deposited on conductor or semiconductor substrates. In CGH fabrication, these are mostly insulator materials that have to be etched. Moreover, microelectronic devices do not always require high-precision manufacturing (e.g. controlled excessive etching and specific process termination are admissible). The fabrication of CGHs places more stringent requirements upon accuracy and, therefore, the equipment and techniques used.

In our opinion, high-frequency reactive ion etching in conjunction with careful etch- depth control can provide the accuracy necessary for CGH manufacturing. Phase levels can be etched one at a time or all in one cycle; the latter technique looks more promising and involves the transfer of a phase relief from the ion-resistant resist layer into the substrate.

Holographic elements that are manufactured by the plasma processing of optical materials have best performance characteristics. However, the sophisticated fabrication process and stringent technical requirements for substrate materials make the cost of CGHs rather high.

The replication of surface reliefs provides a simple way to cheapen the large-scale production of CGHs. The copying technique used in production of laser CDs is best suited to this purpose. The original relief formed in the resist layer is coated with a thin film of conducting material by using, for example, vacuum evaporation. Then, the metal film is thickened to 0.1–0.5 mm by chemical deposition (nickel is usually used for this purpose) and separated from the original element. Before being coated with metal, the resist surface is sometimes coated with antiadhesive material to facilitate the separation. The metal replica, which is an exact copy of the original relief, can now be used as a production master. It is natural that the relief depth must correspond to the refractive index of future elements. One original element is usually used for making a few masters, or the first master is employed to make other masters. Epoxy resins or photopolymer materials are often used for making auxiliary replicas. The first copies are arranged in a single array to provide injection molding of CGHs in optical plastic. This replication methods allows cheap production of CGHs.

4.6 CGH Performance Characteristics

To exemplify the CGH performance, we present the results of the synthesis of laser beamsplitters with different numbers of phase gradation levels. The beamsplitters are designed for $\lambda = 0.633 \mu\text{m}$ and $\lambda = 0.532 \mu\text{m}$ [38]. We used direct e-beam writing to make the phase relief.

Table 1 shows the performance parameters of beamsplitters with 2 to 8 phase levels. They produce diffraction patterns with 4 to 135 equal-intensity beams. Two beamsplitters generate words “IONT” and “MOSCOW” as output patterns. The beamsplitter “EAGLE” gives an eagle-shaped emblem. The diffraction pattern of the beamsplitter “SPEC” is an array of beams of different predefined intensities.

Table 1. Phase multilevel beamsplitters

Output pattern	Number of phase levels	Number of working orders	Efficiency (%)	
			Theory	Experiment
3×11 beams	2	33	79.0	73.3
3×4 beams	2	12	74.8	70.3
“IONT”	3	43	69.5	
“MOSCOW”	3	59	67.8	
“SPEC”	4	14	70.3	
“IONT”	4	43	71.8	69.1
“EAGLE”	4	135	76.1	
2×2 beams	4	4	81.1	
3×11 beams	8	33	86.3	70.5
2×2 beams	8	4	88.2	

Figures 2 and 3 illustrate the work of 3×11 and 3×4 beamsplitters. The laser wavelength is 633 nm, the dimensions of the phase function period is $230.4 \times 230.4 \mu\text{m}$, the aperture of the beamsplitters is $4.61 \times 4.61 \text{ mm}$, which corresponds to 20×20 periods of the phase function. The angle between the neighboring beams is $9.2'$ (3×11 beamsplitter) and $18.4'$ (3×4 beamsplitter). The phase relief depth is 528 nm, the refractive index of resist is 1.6. The efficiency of the beamsplitters are 73.3% and 70.3% respectively. Figure 3d illustrates the use of the 3×4 beamsplitter as an image multiplier.

4.7 Dynamic CGHs

CGHs allow specific stationary patterns in the far diffraction zone. The aim of today’s research is to produce dynamic phase elements allowing real-time control of the diffraction pattern.

We have made efforts to employ acoustic waves in the creation of dynamic beamsplitters. Sound waves are known to cause the index of refraction

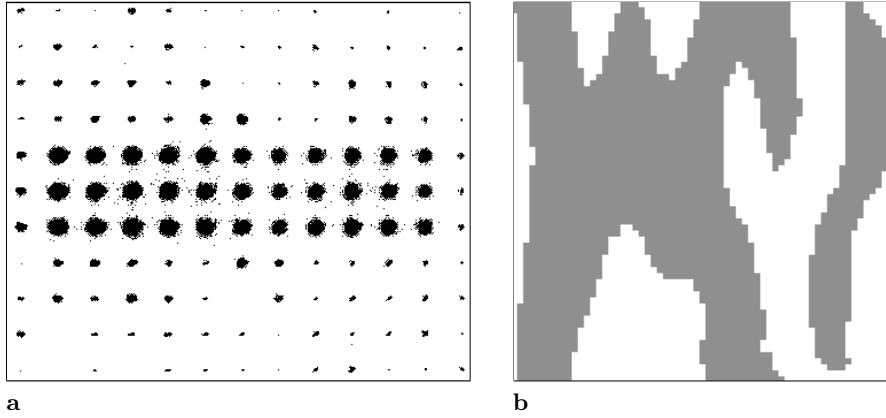


Fig. 2. (a) The output diffraction pattern of a two-level 3×11 beamsplitter. (b) Photograph of one period of the phase structure

of a material to vary sinusoidally. A plane light wave propagating through a material with varied refractive index acquires different phases across the wavefront as if it had encountered a phase diffraction grating on its way. Since two perpendicular low-energy sound waves do not interact, the variations of refractive index add up to produce a superposition of phase diffraction gratings.

We considered the simple case of when two supersonic waves and a light beam propagate in mutually perpendicular directions (Fig. 4). The instant and averaged (over the sound wave period) diffraction patterns were computed. Both traveling and standing acoustic waves were used in the experiment. The amplitude, frequency and phase of sound waves were variables in the computations.

Figure 5a shows the computed diffraction pattern for the case of the acoustic waves of equal amplitudes $A = 0.570\pi$ (0.285λ) (amplitude is given in units representing the maximal phase shift the light wave acquires in passing through the medium in which the given sound wave propagates), and phase difference, $\Delta\phi = 0.5\pi$. The pattern is averaged over the period of the acoustic wave and contains 5 beams of equal intensity (intensity variations are not greater than 1.4%). The computed efficiency of such an acoustic beamsplitter is 69.8%. Decreasing the amplitude of both acoustic waves to $A = 0.45\pi$ (0.225λ) results in the intensity of four outer beams falling to 40% of the intensity of the central beam (Fig. 5b). Figure 5c shows the experimental diffraction pattern corresponding to the computed pattern shown in Fig. 5b.

The experimental acoustic beamsplitter (see Fig. 4) employed LiNbO_3 as the active medium and provided Raman–Natt diffraction, which does not allow high efficiency. It is more promising to work with Bragg diffraction, which can enable not only 100% efficiency but also the control of each diffraction order.

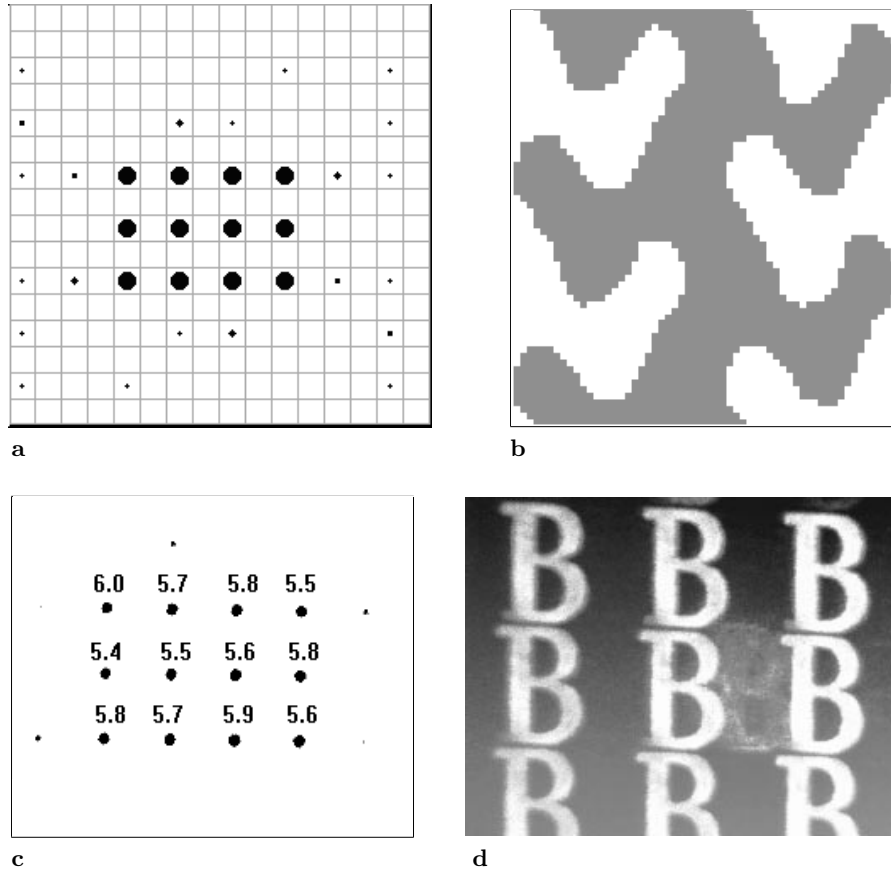


Fig. 3. Two-level 3×4 beamsplitter. The (a) calculated and (c) experimental diffraction pattern. (b) Photo of the phase structure period. (d) The work of the beamsplitter as an image multiplier

Interesting results can be obtained by putting an ordinary CGH immediately or some distance behind the acoustic element. The computations showed that the CGH output pattern in the far diffraction field can be controlled by varying the amplitude and phase of the acoustic waves. When the spacing of the CGH and the sound wavelength are roughly the same, the resulting diffraction pattern becomes highly complicated, and the choice of a particular pattern from all possible solutions rather difficult.

We experimented with the simplest design when a 3×4 two-level beamsplitter was located immediately at the front or back side of the crystal (see Fig. 4). Figure 6 shows the experimental diffraction patterns detected under the following conditions: (a) no acoustic waves are generated; (b) the acoustic wave propagates along the x -axis; (c) the acoustic wave propagates along the y -axis; (d) the computed pattern corresponding to case (c).

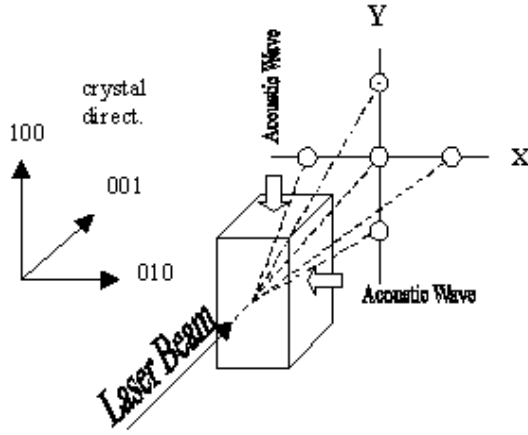


Fig. 4. Two-dimensional acoustic modulator

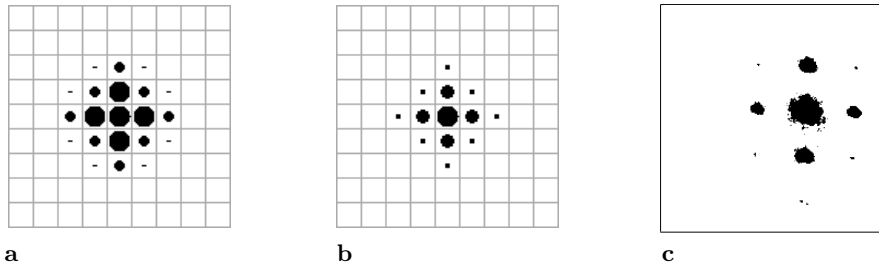


Fig. 5. (a,b) Theoretical and (c) experimental diffraction patterns of the acoustic beamsplitter

It is seen from Fig. 6 that each of the original beams (produced by the stationary 3×4 beamsplitter) is doubled in the coordinate axis parallel to the direction of propagation of the sound wave. It is clear that the location and intensity of beams can be controlled by varying the sound amplitude and wavelength.

Devices such as this may be used in optical switching, for example. An interesting idea is to record a holographic element directly into the LiNbO_3 crystal where the acoustic waves are generated. Another promising design is the integration of a CGH with a device using surface acoustic waves.

5 Conclusion

The paper shows that computer-generated diffractive optics has begun to come to the forefront and replace conventional optics in many fields of application. Advanced computational and manufacturing methods have consider-

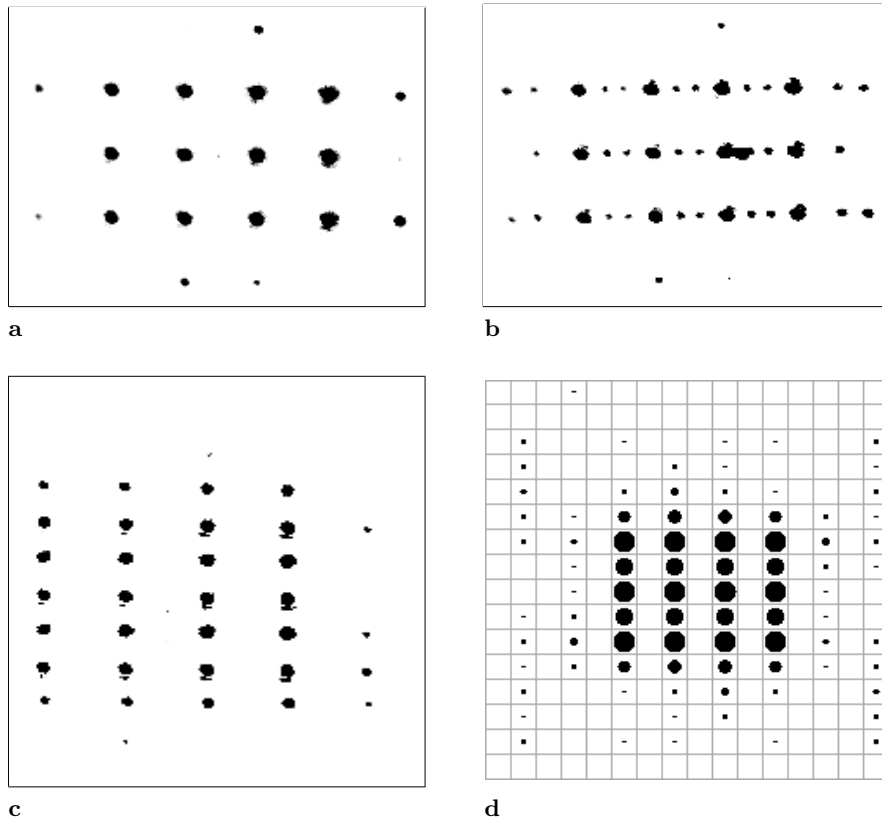


Fig. 6. (a–c) Experimental and (d) computed diffraction patterns of the combined dynamic beamsplitter

ably widened the capabilities of holographic optics and have allowed it the accomplishment of what was earlier impossible.

It is quite predictable that further progress in the theory of diffractive optics will allow the computation of subwavelength structures – highly promising devices for integrated optics. Dynamic CGHs are likely to find use in optical processing and communications. The technology of manufacturing diffractive optics will develop as a separate line of engineering, solving its own specific problems.

References

1. Lessard, R.A., Manivannan, G. (1997) Photochromism used in Holographic Recording: A review. Proc. SPIE 3347, pp. 11–19
2. Counture, J.A., Lessard, R.A. (1997) Organic dye doped colloids solid films used as real-time materials for optical engineering applications. Proc. SPIE 3347, pp. 36–51

3. Barachevsky, V. (1997) Light-sensitive media for high capacity optical memory. Proc. SPIE 3347, pp. 2–9
4. Mikaelian, A.L. (Ed.) (1997) Optical Information Science & Technology '97, Computer and Holographic Optics and Image Processing. 27–30 August 1997, Moscow, Russia. Proc. SPIE 3348
5. Doskolovich, L.L., Perlo, P., Petrova, O.I., Ripetto, P., Soifer, V.A. (1997) Calculation of quantized DOEs on the basis of a continuous series approach. Proc. SPIE 3348, pp. 37–47
6. Kotlyar, V.V., Khonina, S.N. (1997) A method for design of DOE for the generation of contour images. Proc. SPIE 3348, pp. 48–55
7. Soifer, V.A., Pavelyev, V.S., Duparre, M., Ludge, B. (1997) Iterative calculation and technological realization of DOE focusing the laser beam into non-axial radially symmetrical domains. Proc. SPIE 3348, pp. 69–75
8. Prokopenko, S.A., Palagushkin, A.N., Mikaelian, A.L., Kiseliyov, B.S., Shkitin, V.A. (1997) Computation of 2D High-Efficiency Multilevel Phase Beamsplitters. Proc. SPIE 3348, pp. 22–29
9. Volotovskiy, S.G., Kazanskiy, N.L., and Pavelyev, V.S. (1997) Software on iterative calculation and investigations DOE. Computer Optics 17: 48–53
10. Khonina, S.N., Kotlyar, V.V., Lushpin, V.V., Soifer, V.A. (1997) A Method for Design of Composite DOEs for the Generation of Letter Images. Opt Mem Neural Networks 6(3): 213–220
11. Golub, M.A., Duparee, M., Kley, E.B., Kowarschik, R., Ludge, B., Rockstoh, W., Fuchs, H.J. (1996) New diffractive beam shapper generated with aid of e-beam lithography. Opt Eng 35(5): 1400–1406
12. Miller, J.M., Taghizaden, M.R., Turunen, J., Ross, N. (1993) Multilevel-grating array generators: fabrication error analysis and experiments. Appl Optics 32(14): 2519–2525
13. Wong, V.V., Swancon, G.J. (1993) Design and fabrication of a Gaussian fan-out optical interconnect. Appl Optics 32(14): 2502–2510
14. Lalanne, P., Chavel, P. (Eds.) (1993) Perspectives for Parallel Optical Interconnects. Esprit, Basic Research Series, Springer-Verlag, Heidelberg, pp. 85–95
15. Daschner, W., Long, P., Stein, R., Wu, C., Lee, S.H. (1997) Cost-effective mass fabrication of multilevel diffractive optical elements by use of single optical exposure with a grey-scale mask on high-energy beam-sensitive glass. Appl Optics 36(20): 4675–4680
16. Smuk, A.Y., Lawandy, N.M. (1997) Direct laser writing of diffractive optics in glass. Optics Lett 22(13): 1030–1032
17. Chrkashin, V.V., Kharissov, A.A., Korolkov, V.P., Koronkevich, V.P., A.G. Poleshchuk (1997) Accuracy Potential of Circular Laser Writing of DOEs. Proc SPIE 3348, pp. 58–68
18. Perlo, P., Ripetto, M., Sinezi, S., Uspleniev, G.V. (1997) Use circular Laser record system for manufacture grey-scale mask for DOE on the basis of DLW glass plate. Comp Optics 17: 85–90
19. Palagushkin, A.N., Politov, M.V., Prokopenko, S.A., Mikaelian, A.L., Arlamenkov, A.N., Kiseliyov, B.S., Shkitin, V.A. (1997) Fabrication of multilevel HOEs using direct e-beam writing. Proc. SPIE 3348, pp. 76–82
20. Krishnamoorthy, A.V., Xu, F., Ford, J.E., Fainman, Y. (1997) Polarization-controlled multistage switch based on polarization-selective computer-generated holograms. Appl Optics 36(5): 997–1010

21. Fainman, Y., Xu, F., Tyan, R., Sun, P.C., Ford, J.E., Krishnamoorthy, A., Scherer, A. (1997) Multifunctional Diffractive Optics for Optoelectronic System Packaging. Proc. SPIE 3348, pp. 152–162
22. Habraken, S., Michaux, O., Renotte, Y., Lion, Y. (1995) Polarizing holographic beam splitter on photoresist. Optics Lett 20(22): 2348–2350
23. Lima, R.A., Soares, L.L., Cescato, L., Gobbi, A.L. (1997) Reflecting polarizing beam splitter. Optics Lett 22(4): 203–205
24. Wyrowski, F., Kley, E.B., Schnabel, B., Turunen, J., Honkanen, M., Kuittinen, M. (1997) Subwavelength-Structured Interfaces: Fascination and Challenge. Opt Mem Neural Networks 6(4): 231–238
25. dos Santos, J.A.M., Bernardo, L.M. (1997) Quasi sub-wavelength one-dimensional 3x1 array generator for 0.6328 μm . Proc. SPIE 3348, pp. 30–36
26. Honkanen, M., Kettunen, V., Kuittinen, M., Laakkonen, P., Lautanen, J., Turunen, J., Vahimaa, P. (1997) Subwavelength-structured polarization-selective surfaces. Proc. SPIE 3348, pp. 104–107
27. Haritonov, S.I. (1997) Diffraction on quasi-periodical one-dimensional structure. Comp Optics 17: 10–15
28. Huang, Y.T., Su, D.C., Deng, J.S., Chang, J.T. (1997) Holographic polarization-selective and wavelength-selective elements in optic network applications. Proc. SPIE 3348, pp. 2–12
29. Miller, M., Beaucoudrey, N., Chavel, P., Turunen, J., Cambril, E. (1997) Design and fabrication of binary slanted surface-relief gratings for a planar optical interconnection. Appl Optics 36(23): 5717–5727
30. Kamenev, N.N., Nalivaiko, V.I. (1997) Waveguide-hologram-based controllable unidirectional beamsplitter. Proc. SPIE 3348, pp. 140–142
31. Perry, M.D., Boyd, R.D., Britten, J.A., Decker, D., Shore, B.W. (1995) High-efficiency multilayer dielectric diffraction gratings. Optics Lett 20(8): 940–942
32. Brauer, R., Bryngdahl, O. (1997) From evanescent waves to specified diffraction orders. Optics Lett 22(11): 754–756
33. Slinger, C., Brett, P., Hui, V., Monnington, G., Pain, D., Saga, I. (1997) Electrically controllable multiple, active, computer-generated hologram. Optics Lett 22(14): 1113–1115
34. Riza, N.A. (1997) Acusto-optic device-based high-speed high-isolation photonic switching for signal processing. Optics Lett 22(13): 1003–1005
35. Thomas, J.A., Fainman, Y. (1995) Programmable diffractive optical element using a multichannel lanthanum-modified lead zirconate titanate phase modulator. Optics Lett 20(13): 1510–1512
36. Bogomolnyi, V. (1997) To calculation controlled with electrical field elements of optical system on base of metal-dielectric-metal (MDM) structures. Proc. SPIE 3348, pp. 212–217
37. Gerchberg, R.W., Saxton, S.O. (1972) A Practical Algorithm for the Determination of Phase from Image and Diffraction Plane Pictures. Optik 35(2): 237–246
38. Mikaelian, A.L., Prokopenko, S.A., Palagushkin, A.N. (1997) Multilevel Phase Beamsplitters: Design and Fabrication. Opt Mem Neural Networks 6(3): 221–229
39. Prokopenko, S.A., Palagushkin, A.N., Mikaelian, A.N., Kiseliyov, B.S., Shkitin, V.A. (1997) Computer Simulation of 2D Multiple-levels Phase Beam-splitters Fabrication Errors. Proc. SPIE 3348, pp. 83–93